

Fluid viscosity versus solid damping in a cochlear FEM

Xinyu Zhou¹, Daniel Zackon¹ and Torsten Marquardt^{1, a)}

¹*UCL Ear Institute, University College London, 332 Gray's Inn Road, London, WC1X8EE, United Kingdom*

^{a)}Corresponding author: t.marquardt@ucl.ac.uk

Abstract. For reasons of computational efficiency, most cochlear models simulate power dissipation solely by damping inside the solid cochlear partition, disregarding viscous dissipation in the fluid. In recent years, however, simulation incorporating fluid viscosity became reasonably affordable. In this study, we compared the effect of both types of power dissipation using a passive 3D box model implemented in the commercial finite-element modelling (FEM) package COMSOL. Indeed, memory requirements and computation time was approximately 10 time larger when simulating fluid viscosity compared to solid damping only. But the qualitative difference was striking: As expected, when lowering the solid damping in a model without fluid viscosity, the peak of the travelling wave (TW) got higher, moved apically and the apical slope of the TW got much shallower. (I.e., the distance over which the wave amplitude decayed increased substantially.) When lowering the fluid viscosity in a model without solid damping, the peak of the TW also got higher and moved apically, but the slope of decay remained constant. The slope of approximately 30 dB/mm was much steeper than could be achieved with solid damping and compares to the more than 100-dB/octave slopes at the high-frequency side of experimentally measured frequency tuning curves. We conclude that that solid damping cannot replace the computation of viscous dissipation when intending to simulate the sharp TW decay. They have qualitatively different effects.

INTRODUCTION

Fluid-mechanically, the cochlear ducts are small relative to the thickness of the Stokes boundary layer and power dissipation herein are likely to dominate the damping of the travelling wave (TW). But because the simulation of viscous dissipation requires large computational resources, cochlear finite-element models (FEMs) have commonly generated losses in their solid cochlear partition. Although commercial software with thermo-viscous solvers became affordable within the last decade, the mesh density required to resolve the Stokes boundary layers requires a large number of small elements, and therefore, large scale computers. In our experience with COMSOL Multiphysics, just the switching to using its Thermoacoustics Interface increased the requirement for both working memory and computation time by a factor of ten, even with identical mesh density. Thus, we wondered whether expensive simulations with viscous solvers are strictly necessary to simulate a realistic TW.

METHODS

The cochlea was implemented as an uncoiled box with two fluid compartments separated by a 35-mm long solid that represented the cochlear partition (Fig. 3a). The cochlear partition had the density of water, a width of 150 μm at base, 450 μm at the apex and a constant thickness of 10 μm . It was an orthotropic solid with a Young's modulus in the longitudinal direction (E_x) a thousand times smaller than across (E_y). Along the longitudinal location (x), E_y was adjusted to give the model roughly the tonotopy of the human cochlea, resulting for characteristic frequencies above 500 Hz in an octave spacing of roughly 5 mm^{-1} . It was achieved by adjusting empirically the parameter values in the following formula that gives E_y in Pascals. (The distance from the base (x) is given in meter.):

$$E_y = 5 \cdot 10^7 \left(1 - \frac{x}{0.045}\right)^{4.5} \quad (1)$$

The shear moduli were $G_x = (E_y/Pa)/50 \text{ N/m}^2$, $G_y = (E_y/Pa)/10 \text{ N/m}^2$ and $G_z = 1 \text{ N/m}^2$. The corresponding Poisson ratios were $\{0.005, 0.3, 0.005\}$.

A 1.35-mm long compartment with a 0.45-mm wide helicotrema was added to the apical end. The fluid had the mechanical properties of water.

The mesh sectioned the model over the length of the cochlear partition in 700 equal-sized sections. The partition was 1 element thick. The cross-sectional mesh of cochlear partition and fluid compartments was non-uniform to resolve the shear movement within the Stokes boundary layers more finely (see mesh lines in the cross section shown in Fig. 2). Since the model was symmetric (with the cochlear partition and helicotrema symmetrically divided along their midline), all middle surfaces were given a symmetry constraint so that only one-half of the model needed to be solved (450800 elements, 12681661 degrees of freedom).

The acoustic input was applied by defining a perpendicular harmonic displacement to fluid surface above the cochlear partition at longitudinal position zero, thus acting as the oval window (OW). The same fluid surface below the cochlear partition was unconstrained and acted as the round window. Surfaces between fluid and cochlear partition were given a non-slip fluid-structure interaction. The two surfaces next to the solid cochlear partition also had a non-slip constraint. All the outer boundaries of the box had slip constraint because the mesh was here too coarse to resolve the Stokes boundary layers, and thus errors would have occurred when calculating the power flux with a non-slip constrained. Instead, the nodes were used to better resolve the Stokes boundary layers at the cochlear partition, where all of the power dissipation occurs at the TW peak and apical thereof due to the short local wavelength.

Three simulations were run with only viscous dissipation. Both, the bulk and dynamic viscosity of the fluid were set to half, equal and double of that of water at 37°C in these three simulations respectively, while all damping parameter of the solid material were set to zero. Three further simulations were run with the two fluid viscosity parameters set zero, while the value of the six damping parameters (three associated with the tensile and the three with the shear strain of the solid) were adjusted to produce TW envelopes that are most comparable with those obtained with the previous three viscosity settings. All six damping loss factors were here set to the same value, which was 0.0025 in the first, 0.05 in the second and 0.1 in the third simulation. In order to keep the conditions identical, all simulations used the Thermoacoustics Interface, also those with zero viscosity.

The direct stationary solver PARDISO ran on a Dell PowerEdge R910 server (four Xeon CPUs E7- 4870 @ 2.40 GHz, 40 cores total). One of these frequency domain computations took approximately 3 hours, requiring almost all of the available 1 TB RAM.

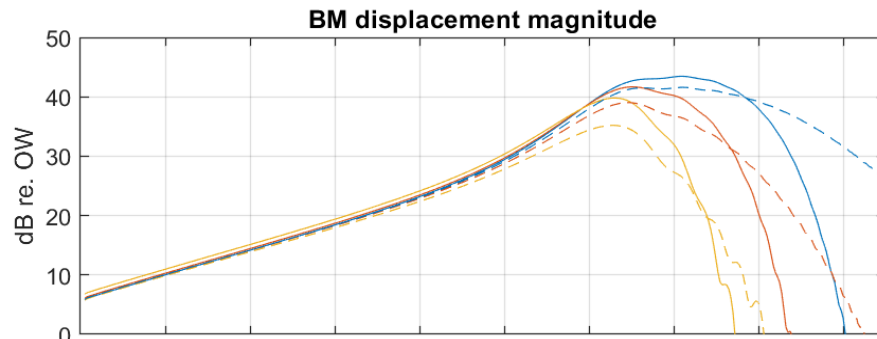
The time-averaged power flux through the cross section at location x was calculated post-hoc as follows²:

$$P_{CS}(x) = \int_0^{L_3} \int_0^{L_2} \frac{1}{T} \int_0^T u \left(p - 2\mu \frac{\partial u}{\partial x} \right) - \mu v \left(\frac{\partial v}{\partial x} + \frac{\partial u}{\partial y} \right) - \mu w \left(\frac{\partial w}{\partial x} + \frac{\partial u}{\partial z} \right) dt dy dz, \quad (2)$$

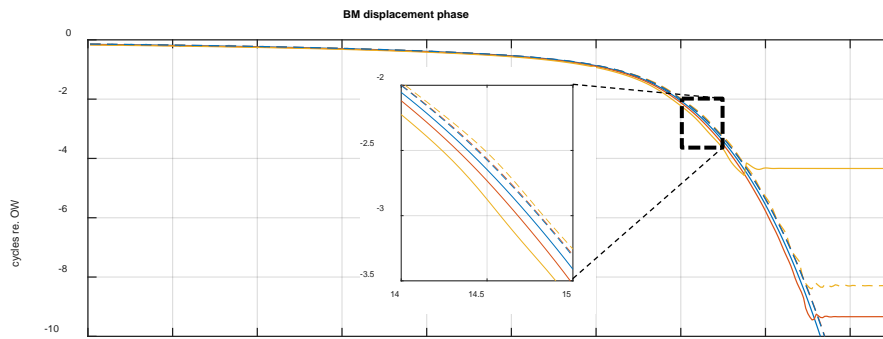
where T is the period of a cycle, μ is the dynamic viscosity, and u , v , and w denote the velocity components in longitudinal (x), radial (y) and transversal (z) directions respectively. L_2 and L_3 are the y - and z -dimensions of the cross section. For this computation, the node density was locally increased to 1- μm resolution utilizing Matlab's *griddedInterpolant* with the modified Akima cubic interpolation method.

RESULTS

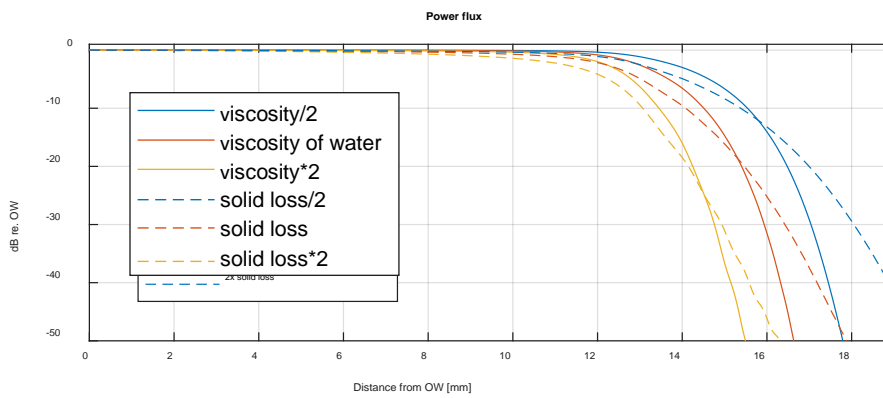
Panel (a) and of Fig. 1 shows the magnitude of the travelling waves as a function of longitudinal location relative to the OW displacement for various values of fluid viscosity while the solid damping was zero (solid lines) and various damping values for the solid material of the cochlear partition while the fluid viscosity was zero (dashed lines). As expected, reduction in the loss parameters cause in both cases the TW peak to move further apically, leading also to only moderate increases in peak amplitude. The decay of the TW shows however striking differences: Overall, it becomes obvious that the solid damping cannot achieve the steep slope produced by viscosity, not even at a cost of 10-dB peak reduction. Second, whereas the slope of the decay becomes shallower when reducing solid damping, the value of fluid viscosity appears to have no effect on its steepness. We will investigate the reason for this further below.



(a)



(b)



(c)

Figure 1. Difference between power dissipation by fluid viscosity (solid lines) and damping within the solid cochlear partition (dashed lines) on magnitude (a), phase (b) and power flux (c) of cochlear TWs. Three parameter values were tested for each type of dissipation (see legend in panel c).

Although at the first glance the type and value of loss does not make a large difference to the TW phase (panel b), the magnified inset reveals that the two types of dissipation have opposite effects: An increase in fluid viscosity slows the TW (i.e., phase accumulation increases), like the TW is facing a higher impedance in apical direction and forces more power to be locally stored in the cochlear partition. On the other hand, an increase in solid damping speeds the wave slightly up, like the increased partition impedance deflects the TW power more along the fluid-filled scalae.

The qualitative difference in power dissipation by solid damping and fluid viscosity becomes most obvious by an analysis of the longitudinal power flux. A comparison of the superimposed graphs in panel (c) reveals that in contrast to the case of solid damping (dashed lines), the TWs with viscous dissipation (solid lines) hardly lose any power before their peaks, but that the power even more rapidly dissipates as the wavelength decreases past the peak. Analogous to the slope of the decaying wave amplitude, the dissipation rate per distance (in dB/mm) is largely independent from the amount of fluid viscosity. In contrast, the rate of power dissipation per distance with solid damping in the solid is proportional to the material's loss factor.

Panel (c) shows clearly that the power has already considerably decreased before the TW reaches its peak, even more so in case damping in the solid than in the fluid. The reason that the TW amplitude is increasing towards its peak despite the power loss is that the power flux focuses more and more on the cochlear partition as the wavelength decreases. This is illustrated in the left column of panels of Fig. 2. They show the power flux density within cross sections at x-positions, where the total power of the three viscous TWs has dropped by 30 dB relative to the input at the OW. The local wavelengths at these three locations are 0.65, 0.4 and 0.35 mm (as can be inferred from the TW phase slope in panel b). It can be seen that the spatial extent of the power flux decreases roughly linearly with local wavelength (in agreement with Lighthill's analytically derived equations for the two-dimensional fluid velocity field²). Because the three cross sections were selected based on equal total power flux, it is obvious that the maximum power densities in these cross sections must differ accordingly. The power density, located close to the cochlear partition, determines its displacement amplitude, which were 20.2 dB, 21.7 dB and 25.6 dB re. OW at these three cross sections (see panel a). In addition, the decrease in cochlear partition stiffness towards the apex contributes to these displacement differences because a higher displacement is required to store the same amount of potential energy at a less stiff location.

The almost identical slopes of the viscous power flux functions at the x-positions (panel c; look where the power has dropped by 30 dB) shows that also the power dissipation is here very similar. (The power drop is 1.28 dB, 1.15 dB and 1.09 dB per 50 μm respectively). To better illustrate this apparent viscosity-independence, the right column of panels in Fig. 2 shows the differences in the spatial distributions of this power dissipation. Dissipation occurs in the Stokes-layer as well as in areas of irrotational-flow fields³. Comparison of panel (b) and panel (f) reveals that decreasing the viscosity by four roughly halves their spatial extent and, consequently, reduces the area to a quarter. This is explained by the facts that the thickness of the Stokes-layer is proportional to the square root of the fluid's viscosity and the spatial extent of the irrotational field is proportional to the local wavelength³, which differs at these two x-positions roughly by a factor of two (see above). At the same time, the labels at the color bars show that the maximum dissipation density differs inversely, roughly also by a factor 4. The reason for the increase in dissipation density (D) is that it grows proportional with the square of the velocity gradient, du/dz :

$$D = \mu \cdot \left(\frac{du}{dz} \right)^2 \quad (3)$$

Two things contribute to the increase in the velocity gradient. First, the reduced spatial extent of the velocity field and, second, the larger displacement of the cochlear partition at the cross section in panel (f), implying that also the longitudinal velocity (u) is 6 dB larger. This means that the term du/dz is a factor of four larger in panel (f) than in panel (b). The effect of its squaring in Eq. 3 is reduced by the fourfold lower dynamic viscosity (μ) in panel (f), so that the power density panel (f) is, taken together, four times that in panel (b) and approximately compensates the fourfold increase in area. In other words, the amount of dissipation in these cross sections is similar and this explains also the before-mentioned viscosity-independence of the rate at which the TW decays apically of its peak when dissipation occurs in the fluid.

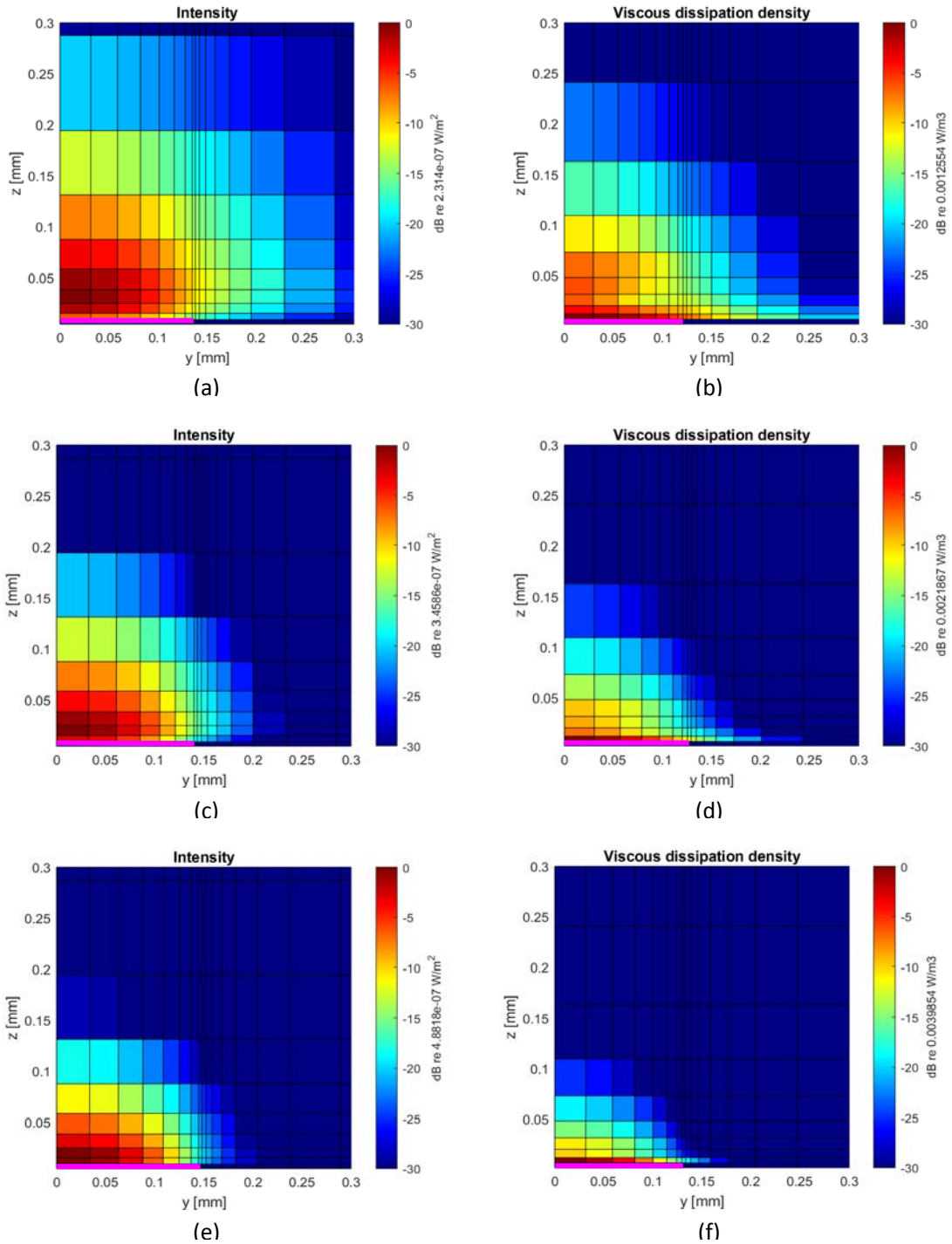


FIGURE 2. Model cross sections showing power flux density (left) and dissipation density (right). Note that only one quadrant of the total cross sections is shown (with the [0,0]-position being the center of the cochlear partition). The panels in the three rows stem from the simulations with the three different viscosity settings. The x-positions of these cross sections are where the power flux has dropped by 30 dB, which are 14.75 mm, 15.95 mm and 17.05 mm from the OW for the first, second and third row respectively. The mesh is finer at the nonslip fluid-solid boundary at the cochlear partition to resolve the Stokes boundary layer and also at the edge of the cochlear partition (which is indicated by the pink bar at the lower left bottom).

DISCUSSION

Already in the 1920's, Bekesy observed the steep slope at which the cochlear travelling wave decays beyond its peak⁴. Later measurements with more sensitive techniques confirmed this steep slope in form of spectral tuning curves with high-frequency slopes exceeding 100 dB/octave^{5,6}, even in post-mortem in human temporal bones^{7,8}. In contrast to the tuning peak, the steepness of this slope is level-invariant, and also stable in its spectral and spatial position. Because normal hearing people have no difficulties understanding loud speech, although the narrow spectral tuning of the active cochlea diminishes quickly with rising sound level, we believe that the sharp tuning at low sound intensities is possibly just an epiphenomenon of preserving sound energy to achieve high displacement amplitude at the characteristic place. Instead, cochlear frequency analysis might be based on the steep and level-independent apical edge of the mechanical excitation pattern – a so far untested proposition.

This FEM study shows that only viscous dissipation can achieve these steep experimentally observed slopes because its effect increases drastically with the decreasing wavelength past the TW peak. The reason behind this wavelength-dependence is that the spatial extent of the fluid viscosity field reduces with the shortening of the TW and is increasingly submerged into the Stokes boundary layer at the cochlear partition where power is rapidly dissipated. It was interesting to observe that the steepness of the TW decay is fairly independent of the fluid's viscosity value. In other words, mechanisms that could potentially reduce the viscous effect by thickening the Stokes boundary layer, and thus, reducing shear velocity⁹ (like the compliant cell layers underneath the basilar membrane), might be able to shift the onset of power dissipation to more apical locations without reducing the final slope of the TW decay.

ACKNOWLEDGMENTS

Xinyu Zhou would like to thank the RNID for his PhD studentship award (S61).

COMMENTS & QUESTIONS

Karl Grosh: We developed an element that takes into account the thickness boundary layer and you can still use inviscid code that quickens up the computation.

Author: I agree it might be possible to speed up the computation by using a kind of phenomenological model that takes the viscous effect on the slope steepness into account. I want to note, however, that Lighthill (1992) demonstrates analytically also areas of viscous loss outside the boundary layer as I have illustrated in my previous MoH contribution.

Sunil Puria: In COMSOL, you can incorporate layers that is viscous and others that are inviscid. That would really speed thing up.

Author: This is a good idea. I already mentioned to Karl, there are also areas of viscous loss in the irrotational-flow fields outside the boundaries that have to be taken into account when doing so.

Sunil Puria: If you have viscosity in the fluid, you can change the high-frequency tuning slope by changing the orthotropic ratio of the cochlear partition.

Author: Yes, I observed this too. The partition needs a high orthotropic ratio so that the wavelength gets sufficiently short, and the extent of velocity field limited to very near the partition. Only this way, the viscous losses increase rapidly to cause the sharp decay in amplitude simulated here. In other words, there must be little longitudinal stiffness coupling so that the wave can slow down.

Audience member: I know it is often approximated that all the viscous losses are in the boundary layer and then the rest of the fluid is inviscid. But it's not. It's an approximation, right? Can you work out with your model how accurate this approximation is?

Author: Correct, I see losses in my simulations also outside the boundary layers. This is illustrated in my figure 2: Losses are almost everywhere in the cross-section where there is energy transport, i.e., fluid is moving, and not restricted to the boundary layer. In the shortwave region, velocity drops sharply with distance from the cochlear

partition, and this gives a lot of fluid shear. Although it is possible to quantitatively compare the losses inside and outside the boundary from the simulation data, I have not yet done this. I agree, this would be interesting.

Renata Sisto: May I add that also in my simulations, viscous losses are in all the fluid volume and is not limited to boundary layers.

Alessandro Altoè: In the longwave region, there is fluid movement and viscous loss also at the outside boundaries, not just at the cochlear partition. Can you quantify these?

Author: I did not resolve the boundary layer there, because I was interested in the sharp decay of the travelling wave and therefore increased instead the mesh density at the partition as much as possible. I knew that the losses in the longwave region are generally small because the volume flow is distributed across the entire cross-section, giving comparatively low fluid velocities. In contrast, fluid velocity in the shortwave region is magnitudes larger because all the volume flow is focused to near the cochlear partition.

REFERENCES

1. D. D. Greenwood, *J. Acoust. Soc. Am.* **87**, 2592–2605 (1990).
2. Y. Wang et al., *Sci Rep* **6**, 19475 (2016).
3. J. Lighthill, *J. Fluid Mech.* **239**, 551–606 (1992).
4. G. von Békésy, *Experiments in Hearing* (McGraw-Hill Book Co, New York, 1960).
5. W. S. Rhode, *J. Acoust. Soc. Am.* **49**, 1218–1231 (1971).
6. M. A. Ruggero et al., *J. Acoust. Soc. Am.* **101**(4), 2151–2163 (1997).
7. T. Gundersen et al., *Acta Otolaryngol.* **86**, 225–232 (1978).
8. S. Stenfelt et al., *Hear. Res.* **181**, 131-143 (2003)
9. M. van der Heijden and A. Vavakou, *Hear Res. Oct* 2:108367 (2021).